

To appear in *The Extragalactic Distance Scale*, M. Livio, M. Donahue and N. Panagia, eds., Cambridge

The I–Band Tully–Fisher Relation and the Hubble Constant

Riccardo Giovanelli

Department of Astronomy and National Astronomy and Ionosphere Center¹, Cornell University,
Ithaca, NY 14953

ABSTRACT

The application of the I band Tully–Fisher relation towards determining the Hubble constant is reviewed, with particular attention to the impact of scatter and bias corrections in the relation. A template relation is derived from galaxies in 24 clusters. A subset of 14 clusters with $cz \sim 4000$ to 9000 km s $^{-1}$ is used as an inertial frame to define the velocity zero point of the relation. Twelve galaxies with Cepheid distances are used to establish the absolute magnitude scale of the Tully–Fisher relation, and thus to determine a value of $H_0 = 70 \pm 5$ km s $^{-1}$ Mpc $^{-1}$. Estimates of the peculiar velocities of the Virgo and Fornax clusters are also given. Assuming that the distance to Fornax is 18.2 Mpc (N1365), $H_0 = 76 \pm 8$ km s $^{-1}$ Mpc $^{-1}$. Assuming that Virgo lies at 17.4 Mpc (M100, N4496, N4639), $H_0 = 67 \pm 8$ km s $^{-1}$ Mpc $^{-1}$.

1. Introduction

The luminosity–linewidth relation has become the most widely used technique for the determination of redshift–independent galaxy distances. While the relationship between kinematic and photometric parameters of spirals was investigated early on by Roberts (1969, 1975), and Ernst Oepik applied it to derive a distance of 450 kpc to M31 in 1922 — a much closer value to the true one than those around 200–250 kpc commonly adopted until the 1950’s —, it is the merit of R.B. Tully and J.R. Fisher (1977) that of forcefully proposing the technique and underscoring its great potential for extragalactic astronomy and cosmology.

The Tully–Fisher (TF) relation was first obtained by correlating blue luminosity and the velocity width of the 21cm line, as observed with telescopes that yield the integrated spectrum of the galaxy, rather than a map of the velocity field. Since the technique requires that target galaxies be fairly inclined in order to minimize the amplitude of the corrections needed to recover the disk’s rotational speed, it was realized early that uncertain corrections for internal extinction

¹The National Astronomy and Ionosphere Center is operated by Cornell University under a cooperative agreement with the National Science Foundation.

of the stellar flux would impose a serious limitation on the method. Aaronson, Huchra and Mould (1980) adopted a photometric datum shifted to the H band, thus drastically reducing the amplitude of, and the error on internal extinction corrections. In the late 1980’s, the advent of CCD devices stimulated the adoption of I and R band as the bandpasses of choice for TF work. Sky background at those wavelengths is relatively low (as compared to H and K bands), detectors have high efficiency and large fields and data acquisition is relatively fast even with small aperture telescopes. The population contributing most of the light at I band is comprised of solar-like stars, several Gyr old. Thus disks are well outlined but of smoother appearance than seen in the bluer parts of the visible spectrum, and their apparent inclinations to the line of sight can be reliably determined. Moreover, processes operating in clusters that may alter the star formation rate in galaxies will have a retarded effect on the red and infrared light of disks; thus, smaller — if any — systematic differences are expected between the TF relation of cluster and that of field galaxies, if I or R band photometry is used (Pierce and Tully 1992). HI single-dish linewidths sample effectively the outer regions of disks and yield values close to twice the asymptotic value of the rotational speed. They are also impervious to uncertainties on major axis position angle. However, not all sky is reachable by large aperture radio telescopes, and velocity widths have also been extensively derived from single-slit spectra, principally targeted at nebular H_α, N and S lines in the red part of the spectrum, and to a lesser extent from H_α Fabry–Perot imaging spectroscopy. HI synthesis imaging has so far had a small impact on this field of work, although the advent of broad-band spectrographs in arrays may make cluster TF work an advantageous proposition.

Much observational and theoretical work has been carried out on the TF relation, and a fair review of even the main individual works is impossible within the space constraints of this presentation. Recent CCD TF work includes the surveys of Pierce and Tully (1988, 1992), Han and Mould (1992), Schommer *et al.* (1993), Mathewson *et al.* (1992), Courteau (1992), Willick (1990), Bernstein *et al.* (1994), Bureau *et al.* (1996) and Giovanelli *et al.* (1996, hereafter G96). By mid-1996, the TF distances of a few thousand galaxies had been estimated, principally with the purpose of determining the characteristics of the peculiar velocity field within $cz \sim 10,000$ km s^{−1}.

The investigation of the peculiar velocity (V_{pec}) field using the TF technique does *not* require an absolute distance calibration of the luminosity–width relation. The observed radial velocity of a galaxy at distance d is

$$cz = H_0 d + [\mathbf{V}_{pec}(\mathbf{d}) - \mathbf{V}_{pec}(0)] \cdot (\mathbf{d}/d) \quad (1)$$

where \mathbf{V}_{pec} is the peculiar velocity vector and $\mathbf{V}_{pec}(0)$ its value at the observer’s location. If the CMB dipole (Kogut *et al.* 1993) is interpreted as a Doppler shift, then in the CMB reference frame $\mathbf{V}_{pec}(0) = 0$. TF yields the distance $H_0 d$ in km s^{−1}. Thus, a template with accurate slope and zero-point is required, such that any galaxy falling on the template can be considered at rest with respect to the comoving reference frame. A *velocity calibration* of the TF zero-point is necessary, which is introduced by assuming that the TF relation of one cluster, or the composite of a set of clusters define $V_{pec} = 0$. Section 4 deals with the process of establishing such calibration. Once

a reliable TF template is in hand, its luminosity scale can be absolutely calibrated by inspecting the location in the TF plane of galaxies with known distances, as obtained via primary indicators. This is equivalent to estimating H_0 .

In this presentation, the physical basis of the TF relation will be reviewed in section 2, in terms of dynamical and scaling arguments. In section 3, the important issue of the scatter about the mean TF relation will be discussed: on it hinge not only the limits of applicability of the technique, but also the impact of bias. Differences in estimate of the latter are largely responsible for wide discrepancies in inferences of both the value of the Hubble constant and the amplitude of peculiar velocities, while the characteristics of scatter affect the issue of whether inverse formulations of the TF relation are bias-free tools. In section 4, the derivation of a template TF relation, from a sample of clusters spread between $cz \sim 1000$ and 10,000 km s⁻¹, will be presented, with emphasis on the treatment of the correction for bias. In sections 5–7, the TF template relation (a) will be calibrated using a set of nearby calibrators with available Cepheid distances and (b) will be used to estimate the Virgo and Fornax clusters' peculiar velocities. These determinations will be used to infer values of H_0 . Throughout this paper, the parametrization $H_0 = 100h$ km s⁻¹ Mpc⁻¹ will be used.

2. The Physical Basis of the TF Relation

There is no detailed physical understanding of the TF relation, the interpretation of which relies on simple scaling relations and dynamical arguments. In the scenario most recently discussed by Eisenstein and Loeb (1996), consider a galaxy of mass M collapsing from a spherical cloud at epoch t_{coll} ; the turnaround radius R_{ta} at that epoch is

$$R_{ta} \propto M^{1/3} t_{coll}^{2/3} \quad (2)$$

according to the spherical collapse model of Gunn and Gott (1972) for $\Lambda = 0$ cosmologies. The total energy of the object after virialization is

$$E \propto M\sigma^2 \propto GM^2/R_{ta} \quad (3)$$

where σ is its velocity dispersion. Assuming that a galaxy results from collapse at a single epoch and not from a succession of mergers, the combination of (2) and (3) yields

$$\sigma \propto (M/t_{coll})^{1/3}, \quad (4)$$

so if all galaxies collapse in single events at the same epoch, and mass-to-light ratios don't vary significantly $L \propto \sigma^3$. Variations in the formation history of galaxy systems should be expected to introduce substantial scatter in the relation, as will be discussed in section 3.

Invoking an alternative set of scaling relations, consider a pure exponential disk of central disk surface brightness $I(0)$ and scale length r_d ; its total luminosity is

$$L_d \propto r_d^2 I(0) \quad (5)$$

On the other hand, the mass internal to radius R is $M(R) \propto RV^2$, and if the rotation curve flattens in the outer regions of the disk as is usually the case for spiral galaxies, the total mass is

$$M_{tot} \propto r_d V_{max}^2 \quad (6)$$

Combining eqns. (5) and (6), we can write

$$L_d \propto (M_{tot}/L_d)^{-2} V_{max}^4 / I(0) \quad (7)$$

If a dark matter halo is present so that the disk mass is $M_d = \Gamma M_{tot}$,

$$L_d \propto (M_d/L_d)^{-2} \Gamma^2 V_{max}^4 / I(0) \quad (8)$$

When a number of “standard” assumptions are made, i.e. that $\Gamma \sim \text{const}$, $M_d/L_d \sim \text{const}$ and $I(0) \sim \text{const}$ (Freeman’s law, 1970), $L_d \propto V_{max}^4$, which resembles the TF relation. In practice, none of the assumptions of constancy for M_d/L_d , Γ and $I(0)$ apply; all those parameters exhibit mild dependencies on V_{max} (or L_d), reducing the exponent to values $n < 4$, in a measure that depends on the adopted photometric band.

Empirical calibrations of the TF relation yield power law behavior as

$$L_d \propto V_{max}^n, \quad (9)$$

with values of $n \sim 3$ in the I band. Some workers (e.g. Aaronson et al. 1986; Willick 1990; Pierce and Tully 1996) have found significant departures from a single power law behavior, and quadratic or bilinear TF fits have been adopted. It has been argued that inappropriate extinction corrections (Giovanelli et al. 1995) or samples including a mixture of morphological types (G96) may result in TF departures from linearity. There is however no *a priori* reason to expect that the TF relation be strictly linear.

3. The Scatter About the TF Relation

In order to correctly infer the predictive power of the TF method and to adequately estimate the amplitude of its biases, a fair understanding of the nature of the associated scatter and its sources is necessary.

The scatter in the TF relation arises from several sources: errors in the *measurement* of TF parameters and uncertainties associated with the *corrections* applied to them combine with *variance in the galactic properties* produced by different formation and evolutive histories, characteristic of each object. The latter is often referred to as the *intrinsic* contribution to scatter, which may appear in the form of velocity field distortions, deviations from disk planarity, other gravitational and disk asymmetries, etc. Several misconceptions regarding the nature of the TF scatter often appear in the literature: that it is well represented by a single number; that the

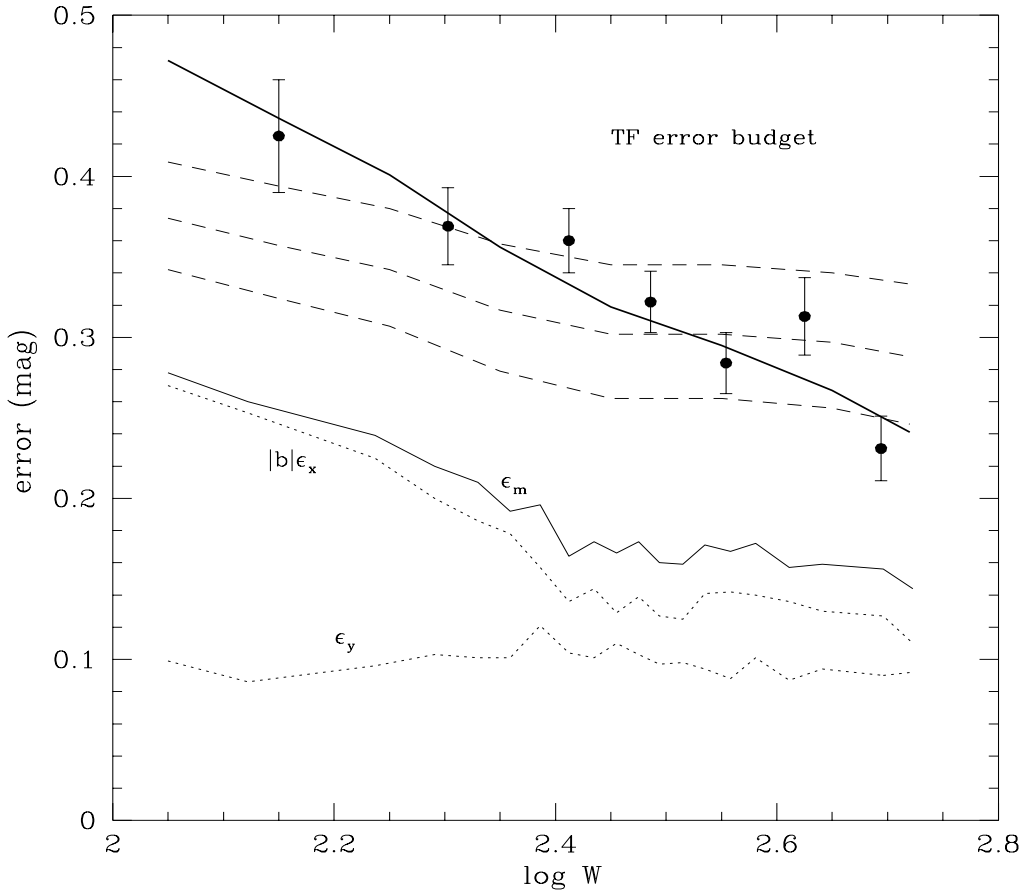


Fig. 1.— Error budget in the TF relation. Mean errors in the measurements and processing of $\log W$ and magnitudes are plotted as dotted lines and respectively labelled ϵ_x and ϵ_y . The total measurement plus processing mean error is labelled ϵ_m . The three dashed lines correspond to the addition in quadrature of the smoothed curve given by ϵ_m and, respectively bottom to top, an intrinsic scatter contribution of 0.20, 0.25 and 0.30 mag. The observed mean r.m.s. scatter is given by the filled symbols and the solid line is a model of the total scatter as given by G96.

measurement and correction errors fully account for the observed dispersion; that only errors on the velocity widths are important. G96 have made a detailed appraisal of the sources of I band TF scatter. Their principal results, illustrated in Figure 1, are:

- (i) *The total TF scatter cannot be represented by a single value; rather, it varies monotonically with the velocity width (luminosity) of the galaxy*, as shown by the solid symbols and the heavy line in Figure 1. Over the range of velocities generally used for TF studies, the r.m.s. scatter in magnitudes varies by a factor of ~ 2 , between 0.5 and 0.25 mag (which translate in distance errors of respectively 25% and 12%). The use of low width objects is not particularly advantageous (see Hoffman & Salpeter 1996). Rather, it is the high width galaxies that generally yield the highest accuracy.
- (ii) *Measurement and processing errors are important contributors to, but they cannot fully account for the amplitude of the total error*. Average errors on the magnitude and on the widths are shown in Figure 1 as dotted lines (that on the width is multiplied by the TF slope so that it can be expressed in mags). It is clear that the *intrinsic* scatter makes an important contribution to the total error budget. Such contribution varies between ~ 0.4 mag for low width objects and ~ 0.2 mag for high width ones. In Figure 1, the *total measurement and processing error*, ϵ_m , which is the result of the combination of magnitude (ϵ_y) and width ($|b|\epsilon_x$, where b is the TF slope) errors, is indicated by a thin, solid line. $|b|\epsilon_x$ and ϵ_y are *not* added in quadrature, because errors in the two coordinates are coupled via inclination corrections.
- (iii) Measurement and processing errors on the magnitude can be important drivers of the scatter, especially for luminous, highly inclined galaxies.

Franx and de Zeeuw (1992) have found that the TF scatter poses strong constraints on the elongation of the gravitational potential in the disk plane of spirals. Their conclusion, that the average ellipticity of the potential in the plane of the disk must be smaller than about 0.06, is reinforced by the scatter amplitude revealed in Figure 1. On the basis of 2.2 μm photometry of 18 face-on spirals, Rix and Zaritsky (1995) find that departures from disk axisymmetry may contribute ~ 0.15 mag to the TF scatter. Their conclusions apply principally to the inner regions of the disk, which are sampled by the K-band observations, and to TF scatter based on optical observations of the rotation field. When the TF relation is based on I band photometry and 21 cm spectroscopy, the Rix & Zaritsky effect becomes of more ambiguous interpretation, as both the light and the HI emission arise in outer regions of disks. Eisenstein and Loeb (1996) estimate that the scatter resulting from varying formation histories of galaxies should exceed 0.3 mag for a broad class of cosmological scenarios. The relatively low values found for the intrinsic scatter in Figure 1 suggest either an unexpectedly late epoch of galaxy formation or that a secular, regularizing feedback mechanism may be responsible for the tightness of the TF relation, as suggested by Silk (1996).

Sandage and collaborators (1994a,b; 1995) advocate for a large value of the TF scatter, near or larger than 0.7 mag, as an explanation for the high values of the Hubble constant resulting

from the use of the TF relation. If the scatter were as large as proposed by that group, large biases would result; their correction would change the zero-point of the TF template relation in the sense that the value of H_0 would be reduced. While the values of the scatter shown in Figure 1 are not as low as advocated by other groups, it appears unlikely that the scatter may be as large as suggested by Sandage *et al.* .

It has been advocated that the use of an *inverse* fit for the TF relation — one where the “independent” variable is the magnitude rather than the velocity width — does away with the need to correct for incompleteness bias (e.g. Schechter 1980). The nature of the TF scatter, especially the fact that velocity width errors can be overshadowed by other sources, weakens the case for a bias-less inverse TF relation.

4. TF Template Relation, Bias and Other Corrections

The construction of a template relation is the most delicate aspect of any TF program. Providing a large number of objects located at a common distance, and therefore exempt from the vagaries introduced by an *a priori* unknown peculiar velocity field in a field galaxy sample, clusters of galaxies are favorite targets for the determination of the properties of the TF relation. They are, however, not exempt from the necessity to evaluate and apply important corrections that take into consideration the interplay between scatter and sample completeness, the non-negligible line-of-sight extent of the cluster, corrections for morphological type mix and others. It is moreover necessary to verify whether a cluster’s environment alters the photometric and kinematical properties of galaxies, so that the derived TF relation for the cluster may not be applicable to the field. In this section, those issues are discussed principally in light of the results obtained by G96, using a sample of galaxies in 24 clusters at cz between 1,000 and 10,000 km s⁻¹ .

4.1. Single Cluster, Basket of Clusters

One commonly-adopted approach to the determination of a TF template relation is to select a single cluster of galaxies as a reference, thereby equating the universal template with the TF relation defined by its members. There are several problems with this approach. In order for the cluster to constrain well the TF slope, a wide dynamic range in each of the TF parameters is desirable, which advocates for the use of a nearby cluster, in which less luminous galaxies can easily be targeted. Such a cluster would, however, yield a highly uncertain zero point, since even a modest V_{pec} would result in a large magnitude offset. Conversely, a distant cluster, for which the latter problem would be minimized, would provide lax constraint for the TF slope. A single cluster sample is moreover unlikely to contain more than two or three dozens of objects, which would produce a template of very poor statistical definition. TF relations of very low scatter are sometimes found in such cases, which reflect far more the capriciousness of small-number statistics

than exceptional data quality. In those cases, low scatter is seldom accompanied by accurate slope and zero-point.

The alternative approach is that of using a set of clusters rather than a single one. More distant clusters in the set can effectively provide an estimate of the velocity zero point, while the nearby ones can help constrain the TF slope. The combination of the various data sets from several clusters does however require the simultaneous estimate of their relative V_{pec} , as well as of the bias and other corrections that apply differentially to each. The procedures followed in obtaining such a combination are discussed as follows.

4.2. The Incompleteness Bias

Much has been written on the ways of estimating the incompleteness bias, which results from the interplay between the degree of completeness of a sample and the amplitude of the TF scatter relation (e.g. Bottinelli *et al.* 1986; Sandage 1994a; Sandage *et al.* 1995; Teerikorpi 1993 and refs. therein). The nature of the bias is illustrated in the simulation shown in Figure 2, where a ‘cluster sample’ is extracted from a population with a luminosity function (LF) as shown by the smooth curve plotted along the vertical axis. The extracted sample is however incomplete, as the histogram of magnitudes superimposed on the LF shows. Incompleteness exhibits a “soft” edge, indicated by the progressive departure of the histogram from the LF. For a flux-limited sample, the histogram would of course track the LF for magnitudes brighter than the limit, then level suddenly to zero. The TF law assigned to the simulated data (UTF) is represented by a dashed line, with a scatter twice as large as that illustrated in Figure 1, averaging about 0.7 mag. The magnified scatter serves to dramatize the bias. A heavy solid line connects filled symbols which identify mean values of the magnitude within bins of velocity width. Incompleteness affects the TF relation derived from the simulated sample in several important ways: (i) the derived slope is less steep than that of the UTF; (ii) the zero-point is brighter than that of the UTF; (iii) the scatter is underestimated with respect to that of the UTF.

Correction recipes for the incompleteness bias have been given in a variety of studies, most recently those by Teerikorpi (1993 and refs. therein), Willick (1994), Sandage *et al.* (1995) and G96. Unlike most other works, which propose analytical or graphic solutions to the problem, G96 give a solution obtained via Monte Carlo simulations, which applies to the case when the TF relation is obtained by fitting magnitude on the logarithm of the velocity width, taking into simultaneous account errors on both coordinates. This case, referred to as the *bivariate* fit, differs from the one usually referred to as the *direct* fit, in which only errors in magnitude are taken into account. The computation of bias corrections does of course depend on the chosen type of fit.

The incompleteness bias generally increases with increasing distance to the cluster. It is principally driven by the amplitude of the TF scatter. An important source of uncertainty in its application is related to the shape of the LF of the galaxy population from which the cluster

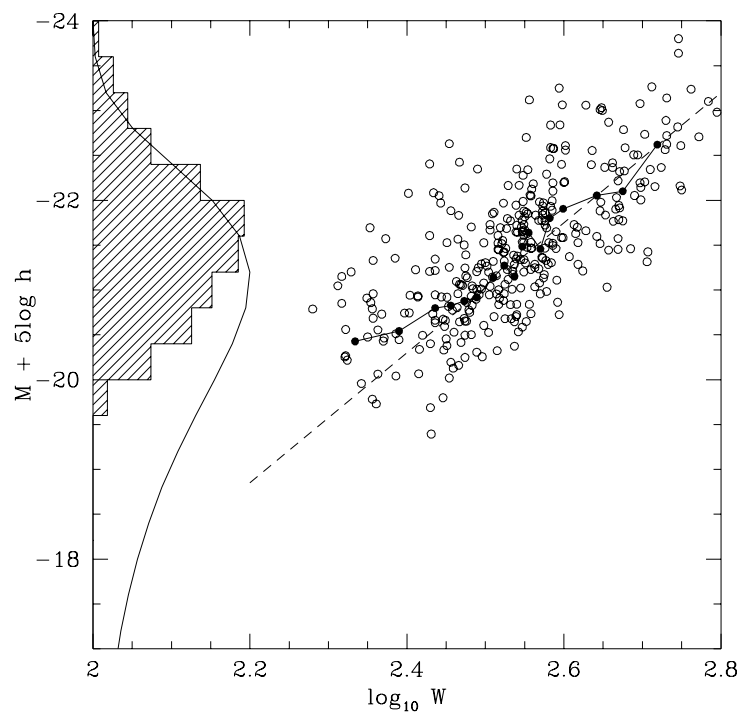


Fig. 2.— Simulated dramatization of the incompleteness bias. See text for explanation.

sample is extracted. G96 estimate that the effect of this uncertainty on that of the TF zero-point is ~ 0.03 mag.

4.3. TF Dependence on Morphology and Cluster Environment

Early work by Roberts (1978), de Vaucouleurs *et al.* (1982) and others showed that in the blue part of the visible spectrum there are significant differences in TF behavior among galaxies of different morphological types. Aaronson and Mould (1983) found such differences to be imperceptible when H band photometry is used. At I band, G96 find a weak but significant difference in the zero point between early- and late-type spirals, Sa and Sab galaxies being less luminous, at a given width, than Sbc and Sc galaxies. Because cluster samples often include a sizable fraction of early-type spirals, an adjustment for the mixing needs to be made.

In Figure 3, the residuals from the I band TF template relation are shown as a function of projected radial distance from the center of clusters. In panels (b) and (c) galaxies are separated between the high and low richness halves of the 24 cluster set of G96, while in panel (a) the total cluster sample is displayed at once. There is no significant evidence of differential TF behavior among spirals, on the basis of their projected cluster location.

4.4. The I Band TF Template Relation

Using 14 clusters with $cz > 4,000$ km s $^{-1}$ to define the zero-point and the whole set of 24 clusters to constrain the slope, G96 obtain a template relation based on the data shown in Figure 4, after the necessary corrections for bias, morphology, cluster extent and peculiar velocity have been applied. The plot includes 555 galaxies. The best bivariate fit is

$$M + 5 \log h = -21.00 \pm 0.02 - (7.67 \pm -0.11)(\log W - 2.5) \quad (10).$$

The statistical errors on the coefficients are small, but as we shall see they are not the principal contributors to the uncertainty of the peculiar velocities inferred using the template.

5. Absolute Calibration of the TF Relation

The final step in the calibration of the TF relation towards deriving an estimate of H_0 relies on the availability of primary distances for galaxies with TF parameters of adequate quality. Such galaxies would be preferably fairly inclined, isolated late spirals, exhibiting no evidence of perturbation in either their light distribution or velocity field. Table 1 lists galaxies with Cepheid distances, that can be potentially used as TF calibrators. Names in various catalogues are listed in cols. (1) to (3) and the morphological type in the RC3 system ('2' stands for Sab, '3' for Sb,

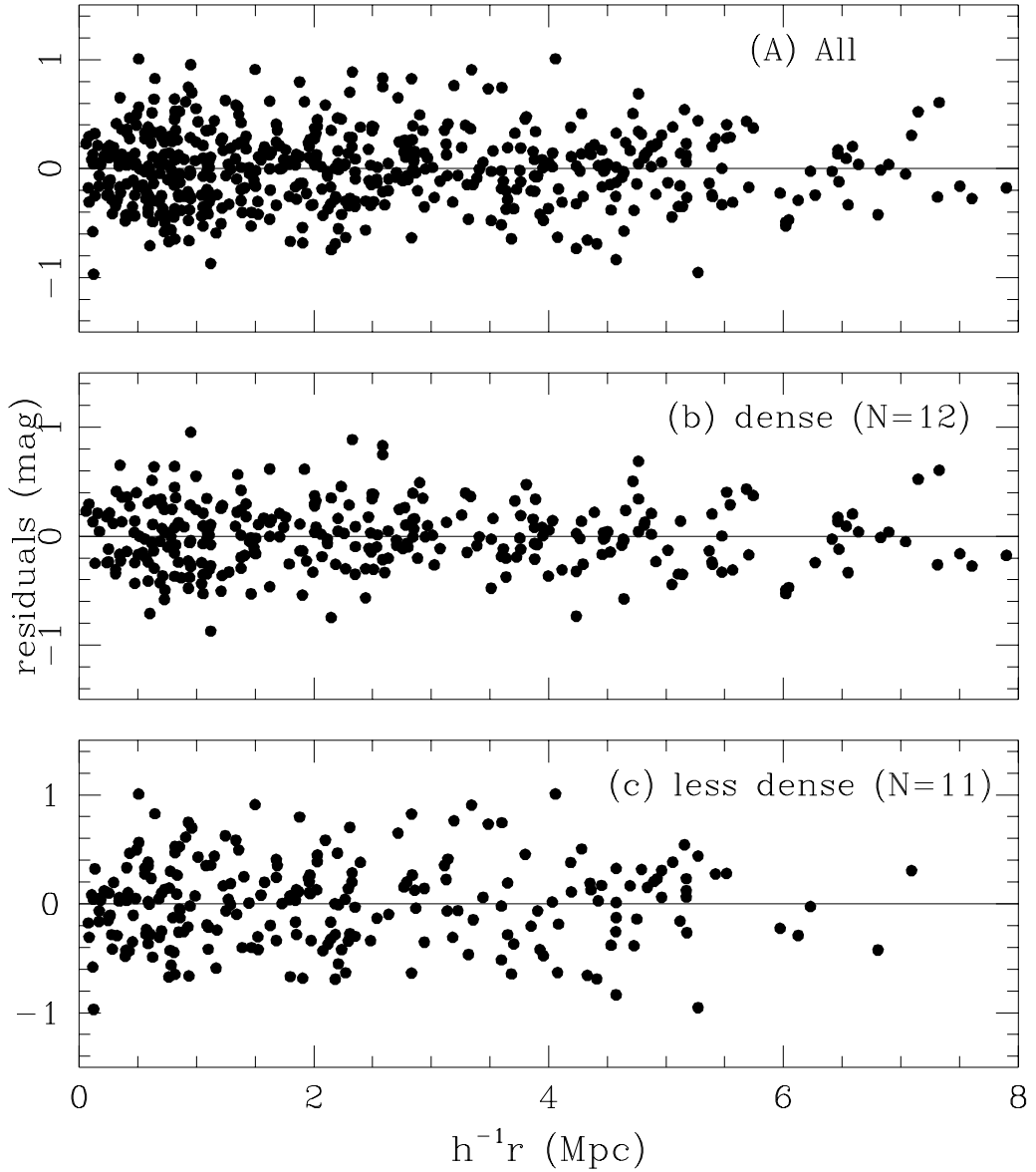


Fig. 3.— TF residuals versus projected radial distance of galaxies from cluster centers. In panel (a), all 555 galaxies in 24 clusters are shown, while in panels (b) and (c) galaxies are separated according to whether they lie in the richer or lower half of the cluster set.

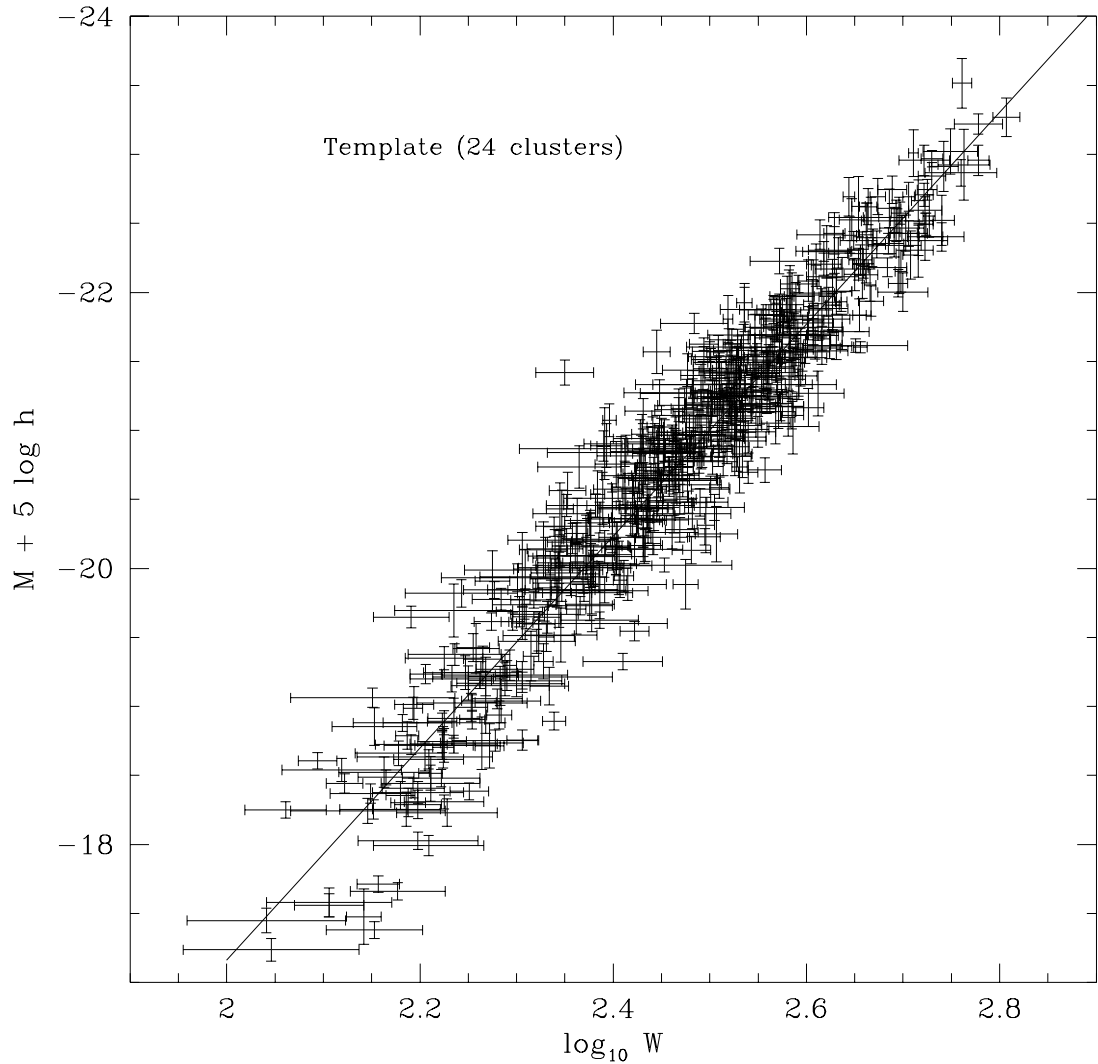


Fig. 4.— Template relation based on 555 galaxies in 24 clusters.

'5' for Sc) is given in col. (4). The adopted inclination of the disk is in col. (5), averaged from various estimates in the literature; the raw, total I band apparent magnitude I_{tot} is listed in col. (6) and the assumed galactic extinction and internal extinction corrections, A_{MW} and A_{int} , are respectively in cols. (7) and (8). The morphological type correction β_{type} , necessary to make the TF behavior of galaxies earlier than Sbc consistent with that of Sbc and Sc objects, is given in col. (9), following the recipe of G96. The adopted distance modulus DM and its estimated error are in col. (10), as given in several recent publications and as presented in this conference. The absolute magnitude, obtained via

$$M_I = I_{tot} - A_{MW} - A_{int} - \beta_{typ} - DM \quad (11)$$

is in col. (11). Its uncertainty, in brackets on the last two significant figures of M_I , has been computed assuming a magnitude measurement uncertainty of 0.1 mag and propagating errors on the extinction correction. The adopted value of the logarithm of the velocity width W and its estimated error are listed in col. (12). The width corresponds to approximate measurements at 50% HI peak flux intensity, after correction for resolution, turbulent motions and inclination effects.

The raw I band magnitudes are from Pierce and Tully (1992) and Pierce (1996), except for NGC 1365, for which we use the average of the Mathewson *et al.* (1992) and of the Bureau *et al.* (1996) values. The spectroscopic data are from a wide variety of sources, too long to itemize here. The velocity widths of large, nearby objects pose accuracy problems of singular nature. Some the data are generally old and unavailable in digital form. In several of the objects, clear distortions are discernible: warps, tidal perturbations and other asymmetries reduce the reliability for TF calibration (e.g. M31, M33 and M81). Other systems are dwarf irregulars (e.g. NGC 2366 and NGC 3109), and thus ill-suited for use with the G96 template which is principally constructed using luminous spirals. Two galaxies (M100 and M101) have very low inclinations and require large and uncertain corrections to the observed widths. One system (NGC 4496) is not only nearly face-on, but a second galaxy is seen superimposed on its disk, making the extraction of photometric parameters highly uncertain. In practice, our estimates of TF parameters are based on a somewhat subjective synthesis of a large amount of heterogeneous material, sometimes involving the measurement of spectra on paper copies of published data figures. Our assignment of error bars to the data are thus reflective of this unorthodox method of parameter derivation, rather than of the original accuracy of the data.

6. The Value of H_0

In Figure 5, the data of all galaxies in table 1 are plotted over a grid of renditions of the template relation, derived as discussed in section 4.4 and shifted according to values of the Hubble parameter ranging between $h = 0.5$ and $h = 1.0$. Keeping the slope of the TF template fixed, we compute the value of h that yields χ^2 minimization of residuals for the set of calibrators.

Table 1. TF Primary Distance Calibrators: Adopted Parameters

UGC	NGC	M	T	<i>i</i>	I_{tot}	A_{gal}	A_{int}	β_{typ}	DM	M_I	$\log W$
(1)	(2)	(3)	(4)	(5)	(6)	(7)	(8)	(9)	(10)	(11)	(12)
454	224	31	3	78	2.18	0.14	0.65	0.10	24.44(12)	-23.15(19)	2.663(39)
20647	300		8	43	7.36	0.02	0.09	0.00	26.66(15)	-19.43(18)	2.269(33)
1117	598	33	5	57	4.98	0.07	0.20	0.00	24.64(10)	-19.92(17)	2.286(32)
1913	925		5	57	9.30	0.11	0.26	0.00	29.86(16)	-20.93(18)	2.330(46)
22699	1365		3	48	8.35	0.00	0.11	0.10	31.30(17)	-23.16(19)	2.684(15)
3851	2366		8	69	11.05	0.07	0.22	0.00	27.68(20)	-16.92(22)	1.887(77)
3918	2403		5	59	7.39	0.06	0.25	0.00	27.51(15)	-20.43(18)	2.389(42)
5318	3031	81	2	57	5.70	0.08	0.28	0.32	27.80(20)	-22.78(18)	2.602(55)
26815	3109		10	80	9.23	0.06	0.35	0.00	25.45(20)	-16.63(22)	2.079(43)
5882	3368	96	2	42	8.10	0.03	0.15	0.32	30.32(16)	-22.72(19)	2.633(34)
7450	4321	100	5	28	8.22	0.02	0.06	0.00	31.04(15)	-22.91(16)	2.681(63)
7668	4496		5	34	10.88	0.00	0.08	0.00	31.13(13)	-20.33(16)	2.412(80)
7732	4536		4	70	9.53	0.01	0.45	0.00	31.11(13)	-22.04(18)	2.489(16)
7884	4639		3	55	10.49	0.02	0.24	0.10	32.00(23)	-21.77(25)	2.534(25)
8981	5457	101	5	21	6.97	0.00	0.04	0.00	29.34(17)	-22.37(15)	2.560(77)

The statistical uncertainty of the derivation, based on the assigned errors to the velocity widths and absolute magnitudes of the calibrators, is small. If we use all the galaxies listed in Table 1, the resulting best fit value is $h = 0.74 \pm 0.02$. However, several of the objects listed in Table 1 are very ill-suited for calibration, as discussed above. After exclusion of N4496 (interacting pair with companion superimposed), N2366 and N3109 (Irregular, low luminosity types), which are identified by unfilled symbols in Figure 5, the best fit yields

$$h = 0.70 \pm 0.02 \quad (12)$$

The formal errors in the statistical analysis given above, of ~ 0.06 mag, arise purely from the errors on the TF parameters of the calibrators, which are likely to be underestimated. Very large galaxies, for example, pose difficulties in the estimation of magnitudes because of problems associated with the determination of the sky brightness level, and the assumed 0.1 mag measurement error may in some cases be too small. Corrections to widths, necessary to bring them to an internally compatible system, as well as commensurable with the data used to obtain the template relation, are also quite uncertain, when the data originate in as heterogenous a set of data sources as in this case. A realistic appraisal of the error arising from measurements and corrections applied to the TF parameters may be significantly larger than the statistical estimates given above. More conservatively than in Table 1, we shall assume that uncertainties in the calibrators' TF parameters contribute $\Delta m_{cal} \sim 0.10$ mag to the error budget.

The error Δm_{cal} does not include the possibility of systematic bias in the zero point of the Cepheid period-luminosity relation and in the determination of the coefficients of the TF template. We deal with the latter uncertainty next.

The statistical accuracy of the TF zero point deriving from the scatter of the 555 data points about the template shown in Figure 4, is ~ 0.02 mag, as given in section 4.4. In addition, two other sources of uncertainty need to be considered: (a) that resulting from the choice of an LF for the computation of the incompleteness bias corrections, which in section 4.2 was estimated to contribute 0.03 mag, and (b) that resulting from the assumption that the set of clusters at $cz > 4000$ km s $^{-1}$ defines a system with $\langle V_{pec} = 0 \rangle$. Part (b) can be estimated as follows. For N randomly selected clusters, located at a mean systemic velocity $\langle cz \rangle$ and characterized by a r.m.s. 1-d peculiar velocity $\langle V_{pec}^2 \rangle^{1/2}$, the magnitude error on the TF zero point obtained by assuming that the set of clusters yields $\langle V_{pec} = 0 \rangle$ is

$$\Delta m \sim 2.17 \langle V_{pec}^2 \rangle^{1/2} \langle cz \rangle^{-1} N^{-1/2} \quad (13)$$

The value of $\langle V_{pec}^2 \rangle^{1/2}$ is quite uncertain. Taking a value intermediate between that suggested by the data of G96 and that required by flat CDM cosmological models (see discussions by Bahcall and Oh 1996 and Moscardini *et al.* 1996), and allowing for a measure of correlation in cluster locations, we obtain $\Delta m \sim 0.06$ mag. The combined uncertainty on the TF zero point is thus $\Delta m_{zp} = (0.06^2 + 0.03^2)^{1/2} \simeq 0.07$ mag.

Combining now in quadrature $\Delta m_{cal} \sim 0.10$ mag, $\Delta m_{zp} \sim 0.07$ and an arbitrarily assumed uncertainty on the Cepheid P-L relation of 0.1 mag, we obtained a total uncertainty of 0.16 mag

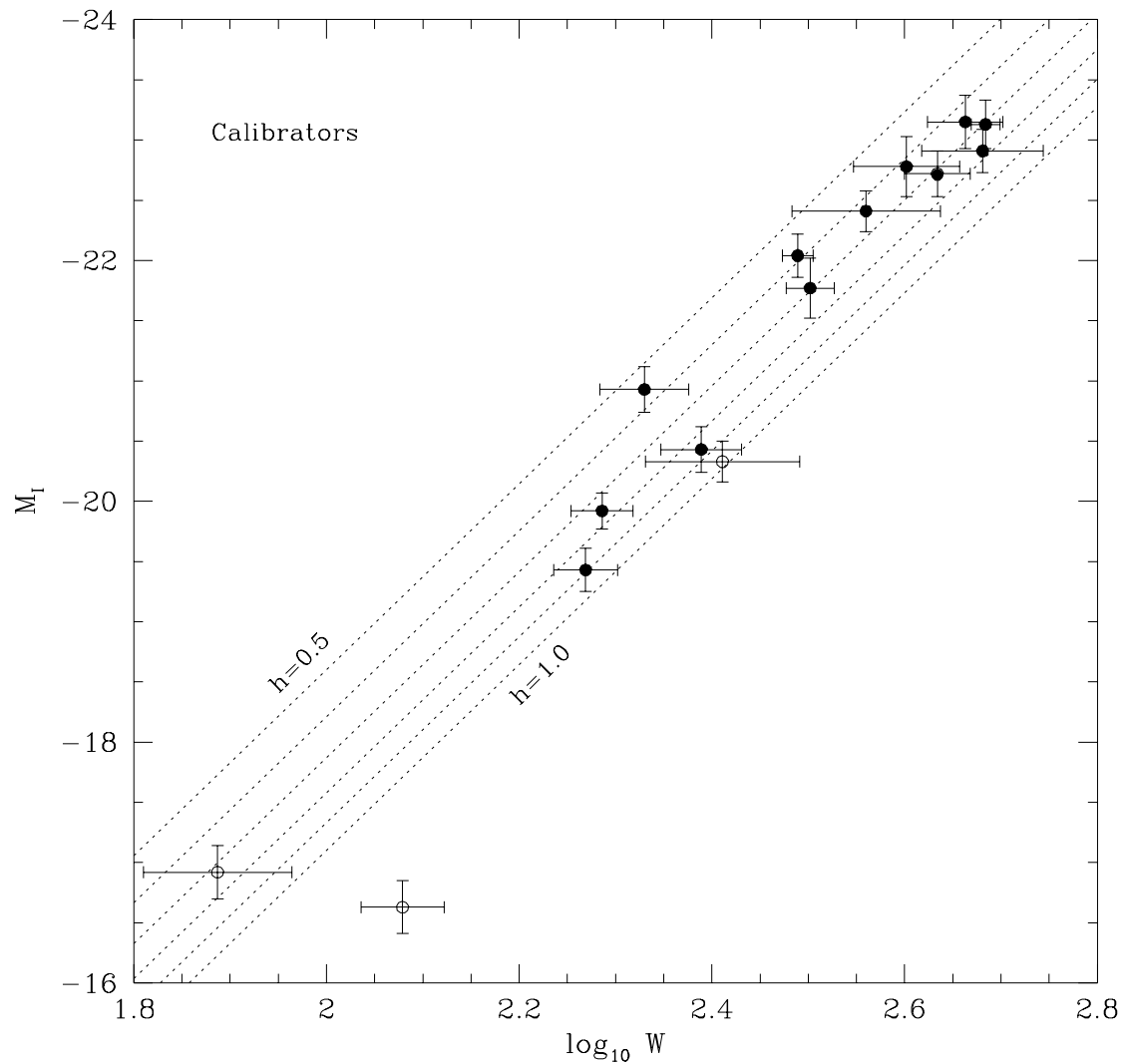


Fig. 5.— TF calibrators with Cepheid distances, superimposed on a grid of TF template relations plotted for different values of h . The unfilled symbols represent galaxies unfit for TF work, as explained in the text.

which, updating expression (12), yields

$$H_0 = 70 \pm 5. \quad (14)$$

7. The Peculiar Velocities of the Virgo and Fornax Clusters

The peculiar velocities of Virgo and Fornax are of particular interest since several of the most recent Cepheid distance determinations correspond to galaxies thought to be members of those clusters. While the route to estimating a value of H_0 via the TF template relation followed in the preceding section is more accurate, it is useful to have at hand estimates of the V_{pec} of the two clusters, which in combination with their systemic velocities and distances can yield local estimates of H_0 . Note that the V_{pec} given here are referred to the same TF template relation used in the preceding section; thus the inferred values of H_0 given below are not fully independent on that given by (14).

Fornax is part of the cluster set of G96. Its V_{pec} , based on a TF sample of 26 galaxies thought to be cluster members and measured in the CMB reference frame, is $-26 \pm 71 \text{ km s}^{-1}$. By expanding the sample to include 13 additional objects thought to be in the cluster periphery, one obtains $V_{pec} = -103 \pm 66 \text{ km s}^{-1}$. Both values assume a systemic recession velocity for the cluster of $1321 \pm 45 \text{ km s}^{-1}$, measured again in the CMB reference frame. If Fornax lies at the distance of NGC 1365, of $18.2 \pm 1.5 \text{ Mpc}$ (Silbermann *et al.* 1996), and if its Hubble velocity $H_0 d = 1385 \text{ km s}^{-1}$, then $H_0 = 76 \pm 8 \text{ km s}^{-1} \text{ Mpc}^{-1}$.

Virgo is not one of the clusters studied by G96. We have, however, used the I band data of Pierce and Tully (1992) and of Pierce (1988), and selected a sample of galaxies reputed to be members of the ‘A’ clump, according to the criteria of Binggeli *et al.* (1985; 1993). Clump A is centered at the position of M87 and has a systemic velocity of $1378 \pm 35 \text{ km s}^{-1}$ (equivalent to a heliocentric velocity of 1050 km s^{-1} as found by Binggeli *et al.* 1993). Twentythree galaxies are used to obtain $V_{pec} = 204 \pm 65 \text{ km s}^{-1}$, following procedures analogous to those described in G96. If Virgo lies at the mean distance of M100, N4496 and N4639 of $17.4 \pm 0.6 \text{ Mpc}$, then $H_0 = 67 \pm 8 \text{ km s}^{-1} \text{ Mpc}^{-1}$.

It is a pleasure to thank Dr. Michael Pierce for generously providing data in advance of publication, help in obtaining the latest Cepheid distances and enjoyable conversations, as well as Dr. M. S. Roberts for providing insights on the velocity field of M31. This research was partially supported by NSF grant AST94-20505.

REFERENCES

Aaronson, M., Mould, J. and Huchra, J. 1980, ApJ 237, 655

Aaronson, M. and Mould, J. 1983, *ApJ* 265, 1

Aaronson, M., Bothun, G.D., Mould, J., Huchra, J., Schommer, R. and Cornell, M. 1986, *ApJ* 302, 536

Bahcall, N.A. and Oh, S.P. 1996, *ApJ* 462, L49

Bernstein, G.M., Guhathakurta, P., Raychaudhury, S., Giovanelli, R., Haynes, M.P., Herter, T. and Vogt, N.P. 1994 *AJ* 107, 1962

Binggeli, B., Sandage, A. and Tammann, G.A. 1985, *AJ* 90, 1681

Binggeli, B., Popescu, C.C. and Tammann, G.A. 1993, *A&A Suppl. Ser.* 98, 275

Bottinelli, L., Gouguenheim, L., Paturel, D. and Teerikorpi, P. 1986, *A&A* 156, 157

Bureau, M., Mould, J.R. and Staveley-Smith, L. 1996, *ApJ* 463, 60

Courteau, S. 1992, Ph. D. Thesis, U. of California, Sta. Cruz

Eisenstein, D.J. and Loeb, A.. 1996, *ApJ* 459, 432

Franx, M. and de Zeeuw, T. 1992, *ApJ* 392, L47.

Freeman, K.C. 1970, *ApJ* 160, 411

Giovanelli, R., Haynes, M.P., Salzer, J.J., Wegner, G., da Costa, L.N. and Freudling, W. 1995, *AJ* 110, 1059

Giovanelli, R., Haynes, M.P., Herter, T., Vogt, N.P., da Costa, L.N., Freudling, W., Salzer, J.J. and Wegner, G. 1996, *AJ* submitted (G96)

Gunn, J.E. and Gott, J.R. 1972, *ApJ* 176, 1

Han, M. and Mould, J.R. 1992, *ApJ* 396, 453

Hoffman, L. and Salpeter, E. 1996, this volume

Kogut, A. et al. 1993, *ApJ* 419, 1

Mathewson, D.S., Ford, V.L. and Buchhorn, M. 1992, *ApJS* 81, 413

Moscardini, L. et al. 1996, preprint

Oepik, E. 1922, *ApJ* 55, 406

Pierce, M. 1996, personal communication

Pierce, M. and Tully, R.B. 1988, *ApJ* 330, 579

Pierce, M. and Tully, R.B. 1992, ApJ 387, 47

Pierce, M. and Tully, R.B. 1996, this volume

Rix, H.-W. and Zaritsky, D. 1995, ApJ 447, 82

Roberts, M.S. 1969, AJ 74, 859

Roberts, M.S. 1975, in Vol. IX, *Stars and Stellar Systems*, ed. by A. Sandage, M. Sandage and J. Kristian, Chicago: U. of Chicago Press, p. 309

Roberts, M.S. 1978, AJ 83, 1026

Sandage, A., Tammann, G. and Federspiel, M. 1995, ApJ 452, 1

Sandage, A. 1994a, ApJ 430, 1

Sandage, A. 1994b, ApJ 430, 13

Schechter, P. 1980, AJ 85, 801

Schommer, R.A., Bothun, G.D., Williams, T.B. and Mould, J.R. 1993, AJ 105, 97

Silbermann, N. et al. 1996, this volume

Silk, J. 1996, in *The Universe at High z , Large Scale Structure and the Cosmic Microwave Background*, E. Martinez-Gonzalez and J.-L. Sanz, eds., Springer-Verlag, in press.

Teerikorpi, P. 1993, A&A 280, 443

Tully, R.B. and Fisher, J.R. 1977, A&A 54, 661

Vaucoleurs, G. de, Buta, R., Bottinelli, L., Gouguenheim, L. and Paturel, G. 1982, ApJ 254, 8

Willick, J.A. 1990, ApJ 351, L5

Willick, J.A. 1994, ApJS 92, 1